the same update rates. For illustrative purposes, the alignment algorithm was applied to simulated data from two sensors that were tracking two common targets. Only one of the targets was used to generate the estimates of the biases, which were then applied to both tracks. Each of the sensors had realistic values for their measurement errors. The filters converged within 30 to 40 s to values of the range, azimuth, elevation, pitch, and roll biases that were close to their actual values. Utilizing these bias estimates, it was possible to obtain a dramatic 24-fold reduction in the alignment error in the xy-plane, but it required at least 40 s before the error in the z-coordinate was reduced. This occurred because of the long time required for the elevation, pitch, and roll bias estimates to converge to their true values. This problem can be reduced by using more than one common target to estimate the biases.

R. E. HELMICK
T. R. RICE
Research and Technology Department
Naval Surface Warfare Center
Dahlgren, VA 22448-5000

REFERENCES

[1] Fischer, W. L., Muehe, C. E., and Cameron, A. G. (1980)
Registration errors in a netted surveillance system.
Report 1980-40, MIT Lincoln Lab, Sept. 1980.

[2] Dana, M. P. (1990)
Registration: A prerequisite for multiple sensor tracking.
In Y. Bar-Shalom, (Ed.), *Multitarget-Multisensor Tracking: Advanced Applications*.
Norwood, MA: Artech House, 1990.

[3] Knicely, R., and Martin, J. (1990)
Multisensor precision tracking study final report.
Report 90-85, Naval Surface Warfare Center, Mar. 1990.

[4] Grindlay, A. (1981)
Radar bias error removal for a multiple site system.
Report 8467, Naval Research Lab, Apr. 1981.

[5] Prather, D. (1981)
Estimation of radar range biases at multiple sites.
Report 8510, Naval Research Lab, Sept. 1981.

[6] Lee, R. H., and Van Vleet, W. B. (1988)
Registration error analysis between dissimilar sensors.
In *Proceedings of SPIE Symposium on Aerospace Sensing (Conference on Sensor Fusion)*, **931**, Orlando, FL, Apr. 1988.

[7] Carlson, G. E., and Bott, M. E. (1973)
Tilt-table alignment for inertial-platform maintenance without a surveyed site.
IEEE Transactions on Aerospace Electronic Systems, **AES-9** (May 1973).

[8] Huang, W. H. (1988)
In-flight observability of gyro reference frame misalignment.
Journal of Guidance, **11**, (May–June 1988).

[9] Wax, M. (1983)
Position location from sensors with position uncertainty.
IEEE Transactions on Aerospace and Electronic Systems, **AES-19**, (Sept. 1983).

[10] Helmick, R. E. (1991)
Alignment of radars with location errors and azimuth misalignments.
In *Proceedings of the 23rd Southeastern Symposium on System Theory*, Columbia, SC, Mar. 1991.

[11] Dela Cruz, E. J., Alouani, A. T., Rice, T. R., and Blair, W. D. (1992)
Sensor registration in multisensor systems.
In *Proceedings of the SPIE Symposium on Aerospace Sensing (Conference on Signal and Data Processing of Small Targets)*, **1698**, Orlando, FL, Apr. 1992.

[12] Goldstein, H. (1980)
Classical Mechanics.
Reading, MA: Addison-Wesley, 1980.

[13] Lewis, F. L. (1986)
Optimal Estimation with an Introduction to Stochastic Control Theory.
New York: Wiley, 1986.

Digital Baseband Processor for the GPS Receiver Modeling and Simulations

A Global Positioning System (GPS) receiver has been modeled mathematically and implemented in software. The digital baseband processor of the receiver performs the maximum likelihood estimations of the GPS observables. The following issues are discussed: 1) the fundamentals of the digital GPS receiver, 2) the modeling of the digital baseband processor, and 3) the performance of the modeled static and dynamic receivers. The software-based receiver is more flexible, less expensive and more accurate compared with hardware receivers in receiver designs and GPS system performance analysis.

I. INTRODUCTION

The NAVSTAR (Navigation Satellite Timing and Ranging) Global Positioning System (GPS) is a satellite-based, worldwide, all-weather navigation and timing system [1]. The GPS is designed to provide precise position, velocity, and timing information on a global common grid system to an unlimited number of suitably equipped users. A GPS receiver is the key for a user to access the system and it has undergone extensive development since the GPS concept was initiated in 1973. The GPS signal structure, the fundamental principles and operations of the receivers, the basic technical approaches to high accuracy and low cost hardware receiver designs are discussed in [2–4]. A functional description of signal processing in the Rogue GPS prototype receiver is presented in

Manuscript received November 17, 1992; revised January 26, 1993.

IEEE Log No. T-AES/29/4/10999.

[5]. The design of a high dynamic GPS receiver using maximum likelihood estimation and frequency tracking is discussed in [6], which pays more attention to the receiver dynamics instead of the receiver cost.

Most of the previous works are dedicated to hardware-based receivers, and hardly any publications are available in the open literature concerning the performance analysis of low-cost GPS receivers and systematic modeling of the receiver functions for the design of software-based receiver systems. Here we develop mathematical modeling of a digital GPS receiver, implement the receiver functions in software and apply the software simulation model to analyze receiver performance and GPS positioning accuracy. Highly digitized receivers are becoming increasingly common in receiver designs. The use of digital receivers simplifies the simulation of the receiver functions on a digital computer and helps to study the performance more accurately. In computer simulations, input GPS signal parameters are known for the purpose of receiver performance analysis and GPS positioning accuracy analysis, which is not possible with hardware-based receivers. The software implementation of the receiver functions is more flexible, less expensive and more accurate compared with hardware implementations in receiver designs and GPS system performance analysis.

This paper is organized as follows. Section II describes the fundamentals of the digital GPS receiver. Section III presents some functional modeling aspects of the digital baseband processor (DBP) of the receiver. Section IV is dedicated to implementation and validation of the receiver simulation model, and to the performance analysis of modeled static and dynamic GPS receivers based on computer simulations. Conclusions of the receiver modeling and simulations are presented in Section V.

II. FUNDAMENTALS OF DIGITAL GPS RECEIVER

A multichannel code correlation receiver operating on the L1-C/A, L1-P, and L2-P signals is shown in Fig. 1. The basic functions of the receiver are to receive the GPS signals from the satellites, to process the input signals, and to provide the GPS observables to a navigation processor. The GPS observables include pseudorange time delay, carrier beat phase, and Doppler frequency shift. Because the navigation message from the satellites plays little role in the applications of the receiver modeling, it is set aside for simplicity in this work. In the RF-IF converters, the L band signals are mixed with the local numerically controlled oscillator (NCO) signals, then the mixed signals are bandpass filtered into the IF signals. The IF signals are amplified and transformed into baseband signals in the IF-baseband converters, with the bandwidth of the low-pass (LP) filter being

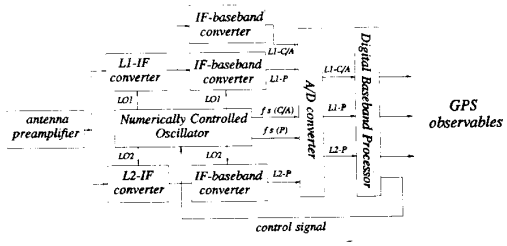

Fig. 1. Block diagram of the digital GPS receiver.

1.023 MHz for the C/A code channel and 10.23 MHz for the P code channels. The three analog signals of the L1-C/A, L1-P, and L2-P channels are sampled in an analog-to-digital (A/D) converter with the sampling rates approximately twice as those of the pseudo-random noise (PRN) code (2.1518 MHz for the C/A code signal and 21.518 MHz for the P code signals), the digital signals are then fed into the DBP where most functions of the receiver are performed.

Consider the input signal (with noise) of a single channel in the DBP

$$r(n) = AP[(1+\zeta)nT_s - \xi T_P] \times \cos[(\omega_b + \omega_d)n + \phi_0] + N(n) \qquad (1)$$

where $P[\cdot]$ is a ± 1-valued PRN code with rate R, delayed by $\tau = \xi T_p$ with respect to GPS system time (T_p is the code chip width), ω_b ($= 2\pi f_b T_s$) and ω_d ($= 2\pi f_d T_s$) are the digital radian frequencies corresponding to the baseband carrier frequency f_b and Doppler shift f_d (T_s is the sampling period), ϕ_0 is the initial carrier phase at $n = 0$, and $N(n)$ is the equivalent input Gaussian noise at baseband. Because of the two-fold impact of the Doppler shift on the received signal (i.e., carrier-frequency offset and code-rate offset), the code rate R is equal to $(1+\zeta)R_0$, where $\zeta = f_d/f_L$ (f_L is the RF frequency), and R_0 is the code rate without the Doppler shift. The A/D converter can be designed to provide high immunity to non-Gaussian interference and jamming, therefore, it is reasonable to assume that the input noise of the DBP is Gaussian band-limited white noise, with the bandwidth determined by the LP filter preceding the A/D converter.

The key functions of the DBP are to provide accurate estimates of the unknown input signal parameters which are the PRN code phase delay ξT_{p_i}, the carrier Doppler shift ω_d and the initial carrier phase ϕ_0. If the signal parameters are assumed to be constant quantities (although unknown) over a sufficiently short observation interval, then one possible approach to the statistical estimations is to seek the maximum-likelihood estimate (MLE) $\hat{\xi}_{\mathrm{ML}}$ of ξ, $\hat{\omega}_{d\mathrm{ML}}$ of ω_d, and $\hat{\phi}_{0\mathrm{ML}}$ of ϕ_0, given N samples of observation $r(n)$, $n = 0,1,\ldots,N-1$ [6]. The MLE of

ϕ_0 and A are

$$\hat{\phi}_0 = -\arg\left\{2A\sum_{n=0}^{N-1} r(n)P[(1+\zeta)nT_s - \xi T_p]e^{j(\omega_b+\omega_d)n}\right\} \tag{2}$$

$$\hat{A} = \frac{2}{N}\left|\sum_{n=0}^{N-1} r(n)P[(1+\zeta)nT_s - \xi T_p]e^{j(\omega_b+\omega_d)n}\right|. \tag{3}$$

With the $\hat{\phi}_0$ and $\hat{A}$ of (2) and (3), the MLE of ξ and ω_d are those values of $\hat{\xi}$ and $\hat{\omega}_d$ which simultaneously maximize the likelihood function

$$L(\xi,\omega_d) \triangleq \frac{1}{N_0}\left|\sum_{n=0}^{N-1} r(n)P[(1+\zeta)nT_s - \xi T_p]e^{j(\omega_b+\omega_d)n}\right|^2. \tag{4}$$

Because of the unique relationship between ζ and ω_d (i.e., $\zeta = \omega_d/2\pi T_s f_L$), $L(\cdot,\cdot)$ is a two-dimensional function of ξ and ω_d. In order to maximize $L(\xi,\omega_d)$, it is necessary to perform the signal acquisition in both time domain ξT_p and frequency domain ω_d. Actually, $L(\xi,\omega_d)$ is equal to $(1/N_0)$ multiplied by the discrete power spectrum of $r(n)\cdot P[(1+\zeta)nT_s - \xi T_p]$ at $\omega = \omega_b + \omega_d$, which can be calculated from the in-phase and quadrature components as follows,

$$\begin{aligned} L(\xi,\omega_d) = {} & \frac{1}{N_0}\left\{\sum_{n=0}^{N-1} r(n)P[(1+\zeta)nT_s - \xi T_p] \right. \\ & \left. \times \cos[(\omega_b+\omega_d)n]\right\}^2 \\ & + \frac{1}{N_0}\left\{\sum_{n=0}^{N-1} r(n)P[(1+\zeta)nT_s - \xi T_p] \right. \\ & \left. \times \sin[(\omega_b+\omega_d)n]\right\}^2. \end{aligned} \tag{5}$$

Therefore, the estimates of the input signal parameters ξ and ω_d may be acquired by noncoherently correlating the N-dimensional observable vector $\mathbf{r}_N$ with the DBP local generated in-phase signal

$$P[(1+\hat{\zeta})nT_s - \hat{\xi}T_p]\cos[(\omega_b+\hat{\omega}_d)n]$$

and quadrature signal

$$P[(1+\hat{\zeta})nT_s - \hat{\xi}T_p]\sin[(\omega_b+\hat{\omega}_d)n],$$

with $\hat{\xi}T_p$ and $\hat{\omega}_d$ sweeping within their own uncertainty domains until the maximum value of $L(\xi,\omega_d)$ is reached.

When the MLEs of ξ and ω_d are acquired and tracked accurately, the input signal is despreaded by the locally generated PRN code (of code phase delay $\hat{\xi}T_p$ and code rate $(1+\hat{\zeta})R_0$). The MLE of

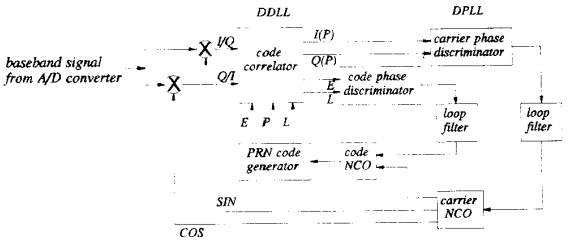

Fig. 2. Simplified block diagram of the DBP.

ϕ_0 may then be obtained from (2) and the carrier phase tracking is performed by a digital phase-locked loop (DPLL). Coherent correlation for tracking code phase and carrier phase is then initiated. Code synchronization and despreading are performed prior to carrier phase tracking since sufficient signal-to-noise ratio (SNR) is necessary for the DPLL to operate successfully. After the PRN code is removed, the signal SNR is increased by the despreading gain. The major components in the DBP are a PRN code phase acquisition system, an early-late digital delay lock loop (DDLL) and a DPLL for each of the L1-C/A, L1-P, L2-P channels, and a data processing system. After the code phase is acquired by a code phase acquisition system, the DDLL provides a measurement of the pseudorange. The input signals of the DDLL are the in-phase (I) and quadrature (Q) signal samples (at a rate f_s) of the baseband GPS signal. The despread I and Q signals then pass to the DPLL (with a much slower rate) for carrier phase synchronization. The DDLL and DPLL loops are inter-connected, the block diagram of which is shown in Fig. 2, where "E", "L", and "P" represent the local early, late, and prompt PRN codes.

III. MODELING OF THE DIGITAL BASEBAND PROCESSOR

Carrier Phase Extraction and Frequency Estimation: For the C/A code channel, after the PRN code of the input signal is removed by the DDLL, the DPLL locks to the code-free carrier signal and outputs the carrier phase tracking residual $\delta\phi$. The data processing system uses the phase residual and the carrier phase of the local oscillator signal to extract the carrier beat phase and to estimate the Doppler frequency shift. The carrier beat phase is extrapolated forward in time to obtain a feedback value (defined as model phase ϕ_n^m) for carrier phase tracking over the next observation interval [5], and the Doppler shift is evaluated based on differencing the successive phase residuals. The received carrier phase ϕ over the nth observation interval is

$$\phi_n = \phi_n^m + \delta\phi_n. \tag{6}$$

The carrier phase variation over the interval is

$$\Delta\phi_n = \phi_n - \phi_{n-1} \tag{7}$$

and the phase variation per sample $\Delta\phi^s_{n+1}$ for the next observation interval is calculated by linearly projecting $\Delta\phi_n$,

$$\Delta\phi^s_{n+1} = \frac{\Delta\phi_n}{N} \tag{8}$$

where N $(= T_n/T_s)$ is the number of the samples in the interval. The initial phase ϕ^i_{n+1} is

$$\phi^i_{n+1} = \phi^{ml}_n + \Delta\phi^s_{n+1} + \delta\phi_n \tag{9}$$

where ϕ^{ml}_n is the model phase of the last sample in the previous interval. The smooth carrier phase transition between two successive observation intervals keeps the DPLL in synchronization with the input carrier signal. The model phase for the $(n+1)$th interval is computed by linearly projecting the model phase of the nth interval,

$$\phi^m_{n+1} = \phi^m_n + \Delta\phi_n. \tag{10}$$

From (6)–(10), the carrier phase extraction can be achieved. The frequency of the received baseband carrier signal is estimated based on the carrier phase residuals from the DPLL. Let f_n be the frequency (assumed to be constant) of the input baseband signal in the nth observation interval, and $\hat{f}_n$ be the estimate of f_n, then the frequency estimation error over the observation interval (T_n) is $\Delta f_n = f_n - \hat{f}_n$. In the absence of noise,

$$\Delta f_n = \frac{\delta\phi_n - \delta\phi_{n-1}}{T_n}. \tag{11}$$

Because of the unavoidable noise contained in the phase residuals, digital filters should be used to reduce the noise effect for low and high dynamic receivers.

Extraction of Pseudorange Time Delay: The receiver obtains the pseudorange time delay by measuring the phase difference between the input PRN code and local generated PRN code. The input PRN code phase is measured by the DDLL. From the GPS signal structure, the code chip rate is proportional to the signal carrier frequency. With the unique relationship between the code rate and carrier frequency, there is a corresponding relationship between the code phase variation and carrier phase variation over each sampling period T_s. The code phase variation of the input PRN code over T_s (in the nth observation interval) is

$$dT = R_n \cdot T_s = \left[R_0 + \frac{f_n - f_b}{1540}\right] \cdot T_s \tag{12}$$

where R_n is the code rate in the interval. Equation (12) can be written as

$$dT = R_0 \cdot (T_s - \Delta\tau^b_n) \tag{13}$$

where $\Delta\tau^b_n$ is the time delay variation per sample,

$$\Delta\tau^b_n = \frac{f_b - f_n}{f_L} \cdot T_s = -\frac{f_n - f_b}{1540} \cdot \frac{1}{R_0} \cdot T_s \tag{14}$$

for the L1 channels. Equations (12) and (13) describe two ways to get the input code phase variation. The first equation represents dT with the changing code rate and constant time duration T_s; the second equation represents dT with the constant code rate R_0 and instantaneous time delay variation of the input code signal.

The noise error is one of the dominant errors in GPS pseudorange measurements. One way to reduce the noise error is to narrow the bandwidth of the DDLL, which, on the other hand, dramatically increases the code phase tracking error due to the receiver dynamics. Another efficient technique (carrier-aiding technique) uses the carrier phase to aid the code phase tracking loop. A DPLL with appropriate bandwidth should track the carrier phase of a dynamic system and, at the same time, produce responsive integrated phase, representing an accurate variation in pseudorange time delay when properly scaled. If the variation in pseudorange time delay is continuous, the bandwidth of the DDLL may be significantly narrowed to reduce the noise error. Consequently, the DPLL provides accurate time delay variations, while the DDLL resolves the ambiguity in the time delay, which results in a significant improvement in accuracy over code only operation. From the definition of the Doppler shift, we may deduce that the time delay variation (in second) over the nth observation interval is

$$\Delta\tau_n = \frac{f_b}{f_L} \cdot T_n - \frac{1}{f_L} \cdot \Delta\phi_n \tag{15}$$

where $\Delta\phi_n$ is the carrier phase variation (in cycle) over the observation interval T_n. For example, in the C/A code channel, if the DDLL is closed every k ms, that is, $T_n = k$ ms, $f_b = 17.248$ kHz, $f_L = 1575.42$ MHz, then from (15), the time delay variation over the interval is

$$\begin{aligned}\Delta\tau_n &= \frac{17.248 \cdot k - \Delta\phi_n}{1575.42} \quad (\mu s) \\ &= \frac{17.248 \cdot k - \Delta\phi_n}{1540} \quad \text{(C/A code chips)}.\end{aligned} \tag{16}$$

With the carrier aiding, the time delay error due to the carrier phase tracking error is very small if the DPLL locks to the input carrier phase. The local C/A code keeps in step with the input code signal by changing the incremental code phase over each sample period in the interval. Because of the error in the frequency estimation, there also exists an error in the code rate estimation. Furthermore, due to the dispersion of the signal propagation media from the satellite to the receiver, the signal group delay (i.e., the code phase delay) is offset from the carrier phase delay. Consequently, the code phase residual from the DDLL is used to correct the carrier-aided code phase synchronization over a certain period.

TABLE I
Errors in the GPS Observables with a 2nd-Order DPLL

(C/N_0), G_1, R[7], T_n = 20 ms	Carrier Phase Error (cycle)		Code Phase Error (code chip)		Frequency Error (Hz)	
	mean	variance	mean	variance	mean	variance
40 dB-Hz, 0.6, 2.0	5.67E-7	3.41E-4	7.13E-4	8.14E-5	5.48E-3	1.40E-2
40 dB-Hz, 0.8, 2.0	−5.67E-7	4.65E-4	4.67E-4	1.35E-4	5.58E-3	1.81E-2
40 dB-Hz, 1.0, 2.0	6.00E-7	7.56E-4	5.53E-4	1.45E-4	4.99E-3	1.81E-2
40 dB-Hz, 0.8, 1.5	−3.67E-7	3.10E-4	4.57E-4	1.32E-4	5.76E-3	1.78E-2
40 dB-Hz, 0.8, 2.5	6.67E-8	7.28E-4	5.70E-4	1.45E-4	5.23E-3	1.82E-2
35 dB-Hz, 0.8, 2.0	−9.83E-6	1.48E-3	8.37E-4	3.30E-4	5.83E-3	2.02E-2
45 dB-Hz, 0.8, 2.0	1.00E-6	1.45E-4	2.35E-4	4.15E-5	5.60E-3	1.75E-2

TABLE II
Errors in the GPS Observables with a 3rd-Order DPLL

(C/N_0), G_1, R = 2.0, P = 3.0[7], T_n = 20 ms	Carrier Phase Error (cycle)		Code Phase Error (code chip)		Frequency Error (Hz)	
	mean	variance	mean	variance	mean	variance
40 dB-Hz, 0.8	1.35E-5	1.21E-3	−1.28E-3	2.82E-5	5.73E-3	2.10E-2
40 dB-Hz, 0.9	1.83E-6	1.54E-3	8.75E-4	9.76E-5	8.03E-3	3.00E-2
40 dB-Hz, 1.0	6.00E-6	2.52E-3	−7.75E-4	2.95E-5	7.22E-3	3.08E-2
35 dB-Hz, 0.8	−6.50E-6	3.91E-3	−1.94E-3	7.28E-5	4.84E-3	2.88E-2
45 dB-Hz, 0.8	6.87E-7	3.78E-4	−7.70E-4	9.63E-6	5.66E-3	1.84E-2

Complete modeling of the digital receiver can be found in [7], which includes the modeling of the DDLL and DPLL, the signal processing of the P code channels and the least-squares fitting of the GPS observables to reduce the receiver output data rate.

IV. RECEIVER PERFORMANCE ANALYSIS BY COMPUTER SIMULATIONS

The discrete nature of the digital receiver makes it possible to simulate the receiver functions directly on a computer. To perform the computer simulations, we need to simulate input GPS signals. A Keplerian satellite orbit is assumed, whose properties are constant with time and could be described by the satellite broadcast ephemeris parameters and the ephemeris reference time. From the satellite orbit, the satellite position and velocity may be calculated. Then by choosing dynamic patterns of the receiver, the signal propagation time delay, carrier phase delay, and Doppler frequency shift can be computed. Combining with software PRN code generators and Gaussian noise generators, the input GPS signals with noise are generated in software. The details of the implementation and validation of the computer simulation model of the input signal generator and the receiver have been discussed in [7].

Performance of Static Receivers: For a static receiver, the variations of the input signal parameters result only from the satellite dynamics. With an example of the satellite orbit data obtained from hardware receiver measurements, the variation rates of input signal parameters are very smooth compared with the bandwidth of the DDLL and DPLL, so that the errors of the observables result primarily from the input noise. Tables I and II show the mean values and variances of the GPS observable errors for the L1-C/A channel based on a 30 s period of coherent code phase tracking (with carrier aiding) and coherent carrier phase tracking with the observation interval T_n = 20 ms. A 1st-order DDLL (with the loop filter gain G_1 the same as that of the DPLL) is used for code phase tracking and a 3rd-order DPLL is used for the carrier phase tracking and frequency estimation. After the local NCO locks to the input carrier signal, the carrier-aiding technique is used for PRN code phase tracking with the code phase delay being updated every 1 s by the coherent DDLL. The accuracy of the GPS observable measurements depends on the input signal parameters (the carrier-to-noise density ratio C/N_0 and the system dynamic parameters), the receiver design structures (the loop orders of the DDLL and DPLL) and design parameters (the loop filter gains, sampling frequencies, the observation interval, etc.). Hence, the performance of a GPS receiver may be described by the receiver system noise errors under certain receiver design conditions. The modeled software receiver performance is compared with that of the Rogue receiver [5]. Given nominal C/N_0 values of the input signals, a 5 min correlation interval, a 125 K system temperature and an antenna gain of 3 dB, the Rogue receiver has a P code phase tracking error equal to or less than 1 cm and a carrier phase tracking error less than 0.01 cm. Under the same conditions, the modeled software receiver has a P code phase tracking error less than 0.15 cm and a carrier

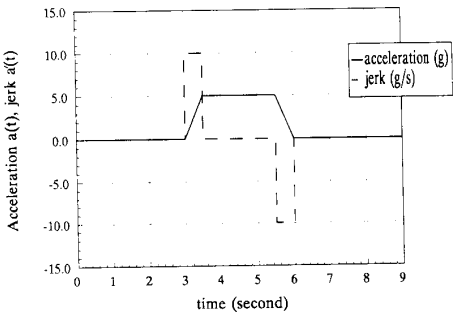

Fig. 3. Receiver dynamic pattern.

phase tracking error less than 0.001 cm. The reasons that the software receiver has better performance are: 1) the sampling rates of the modeled receiver are higher than those of the Rogue receiver; 2) in the high-speed code correlators of the DDLL, the signals are represented by "float" variables of single precision in the software receiver, which are quantized to only three levels in the Rogue receiver; 3) the functions of the hardware circuitry are idealized in the software modeling.

Performance of Dynamic Receivers: It is expensive to analyze the performance of dynamic hardware receivers, especially in the cases of high dynamics. It may be difficult to accurately control and measure the motions of the highly dynamic receivers. Computer simulations are a much simpler approach. Here, for the reason of simplicity, we assume that: 1) the initial velocity of the receiver is zero; 2) the vector of the receiver velocity is in the direction opposite to that of the distance vector from the receiver to the satellite; 3) the receiver dynamics do not change the elevation angle of the satellite as viewed from the receiver. It should be mentioned that the simulation model can be applied to analyze the cases without the above assumptions, should the parameter variations of the input GPS signals be modeled appropriately. Fig. 3 shows the receiver dynamic pattern [6]. We choose the pattern because of the high-speed variations of the acceleration and its derivatives (both the first order and higher orders). Fig. 4 presents the simulation results of the GPS observable errors from the C/A code channel with a 1st-order carrier-aiding DDLL and a 3rd-order DPLL. The simulation parameters are: the maximum acceleration of the receiver $A = 49.0$ m/s^2, $C/N_0 = 40$ dB-Hz, $T_n = 20$ ms, the DDLL loop filter gain $G_1 = 0.4$, the DPLL loop filter parameters $G_1 = 0.8$, $R = 2.0$, $P = 3.0$ [7]. The code phase is modified every 0.5 s by the coherent DDLL with carrier aiding. We observe that the initial code phase tracking error (from the DDLL without carrier aiding) decreases after the carrier-aiding technique is used. Computer simulations are also performed with other receiver dynamic pattern and parameters, DPLL structures and parameters, the durations of the observation interval

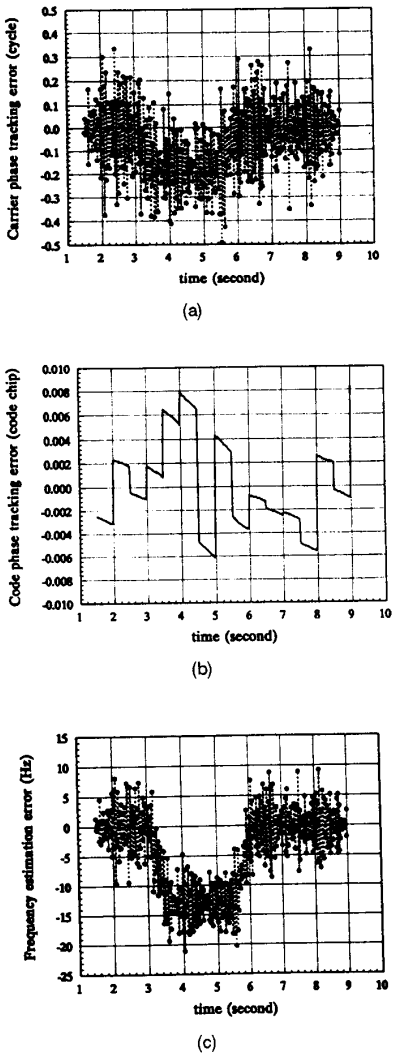

Fig. 4. GPS observable errors of dynamic receiver. (a) Carrier phase tracking error. (b) Code phase tracking error. (c) Frequency estimation error.

and carrier-to-noise density ratios of the input signals. From Fig. 4 and other simulation results in [7], we can conclude that: 1) the frequency estimation error and the carrier phase tracking error have the same pattern as that of the acceleration of the receiver but vary in the opposite direction; 2) with the carrier-aiding technique, code phase tracking error is very small as long as the local carrier NCO is not out of step with the input carrier phase and frequency; 3) the frequency estimation is very important in the case of high system dynamics—the higher the rate of the input frequency estimation update, the better the receiver dynamic performance; and 4) in the case of low system dynamics, the lower rate of the input frequency estimation update is better for reducing the frequency estimation noise.

V. CONCLUSIONS

We have presented the fundamentals and functional modeling of the software-based digital GPS receiver. The developed simulation model has been used to study the performance of the modeled static and dynamic receivers. The accuracy of the GPS observables are functions of the (C/N_0) values of the input signals, the system dynamics, receiver design parameters, and the signal processing algorithms of the DBP. The significance of this work is the advantages of the modeled software receiver over hardware-based receivers in analyzing the effects of the receiver design parameters, the system (including both the satellites and the receiver) dynamics and the signal propagation media (such as ionosphere, troposphere, multipath [8], GPS antenna, etc.) on the GPS observables. Compared with the software method, the theoretical analysis or hardware methods may be very difficult, inaccurate, or prohibitively costly.

This work may be extended in designing a software interface between the receiver and a data processor or navigation processor which will make it possible to transform the GPS observables into the point positioning information. Furthermore, if multiple receivers are modeled, then with linear combinations of the observables, simulations of relative positioning may be performed, such as (between-epoch, between-receiver or between-satellite) single and double differences.

WEIHUA ZHUANG
Telecommunications Research Laboratories
800 Park Plaza, 10611-98 Avenue
Edmonton, Alberta
Canada T5K 2P7

JAMES TRANQUILLA
Department of Electrical Engineering
University of New Brunswick
Fredericton, NB
Canada E3B 5A3

REFERENCES

[1] Parkinson, B. W., and Gilbert, S. W. (1983)
NAVSTAR: Global positioning system—Ten years later.
Proceedings of the IEEE, **71** 10 (Oct. 1983), 1177–1186.

[2] Ward, P. (1980)
An advanced NAVSTAR GPS multiplex receiver.
Presented at the IEEE 1980 Position Location And Navigation Symposium, Atlantic City, NJ, 1980.

[3] Scherrer, R. (1985)
The WM GPS Primer.
Wild-Magnavox Satellite Survey Co., Heerbrugg, Switzerland, 1985.

[4] Ould, P. C., and Van Wechel, R. J. (1981)
All-digital GPS receiver mechanization.
Journal of the Institute of Navigation, **28**, 3 (Fall 1981), 178–188.

[5] Thomas, J. B. (1988)
Functional description of signal processing in the rogue GPS receiver.
Publication 88-15, Jet Propulsion Laboratory, Pasadena, CA, June 1988.

[6] Hurd, W. J., Statman, J. I., and Vilnrotter, V. A. (1987)
High dynamic GPS receiver using maximum likelihood estimation and frequency tracking.
IEEE Transactions on Aerospace and Electronic Systems, **AES-23**, 4 (July 1987), 425–437.

[7] Zhuang, W. (1992)
Composite GPS receiver modelling, simulations and applications.
Ph.D. dissertation, Department of Electrical Engineering, University of New Brunswick, Fredericton, Oct. 1992.

[8] Zhuang, W., and Tranquilla, J. (1992)
Multipath effects on the GPS observables.
In *Proceedings of the Sixteenth Biennial Symposium on Communications*, Kingston, Ontario, Canada, May 1992, 454–457.

A Series Representation of the Spherical Error Probability Integral

This paper derives an infinite series representation of the spherical error probability integral (SEPI). The SEPI characterizes missile miss distance distributions resulting from Monte-Carlo simulations. The SEPI is used when these distributions occupy a three-dimensional region of space. Truncation of this series provides a computationally efficient tool for approximating the SEPI. A series covergence analysis is presented which provides an upper bound on the approximation accuracy. The accuracy bound may be used to determine a sufficient number of terms needed for approximation to any desired accuracy. Presentation of numerical results provides empirical confirmation of the validity of the series expression. Calculation of the truncated series and numerical integration of the SEPI generate the numerical results. It is shown that the SEPI converges to the circular error probability integral as the standard deviation of a given component approaches zero. Approximation error bounds, as a function of sigma, are derived.

I. INTRODUCTION

Missile system performance analysis often uses CEP (circular error probable) as a measure of miss distance distribution. The CEP gives the radius of a circle in which there is a 50% probability that a realization of the Gaussian random miss vector resides within this circle. The circle is centered at the mean miss. Use of the CEP assumes that the miss distribution exists in a planar region. When exercising a missile system simulation in a Monte-Carlo fashion

Manuscript received October 25, 1992.

IEEE Log No. T-AES/29/4/10996.